Journal of Rehabilitation in Civil Engineering 4-2 (2016) 01-24

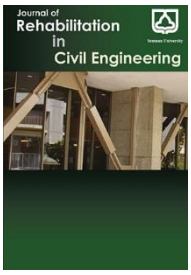

journal homepage: http://civiljournal.semnan.ac.ir/

Characteristics of Horizontal and Vertical Near-Field Ground Motions and Investigation of Their Effects on the Dynamic Response of Bridges

M. M. Memarpour[1], G. Ghodrati Amiri[2*], H. Razeghi[2], M. Akbarzadeh[2], A. Tajik Davoudi[2]

1. Civil Engineering Department, Faculty of Engineering, Imam Khomeini International University, Qazvin, Iran
2. Center of Excellence for Fundamental Studies in Structural Engineering, College of Civil Engineering, Iran University of Science and Technology, Narmak, Tehran, Iran

Corresponding author: *ghodrati@iust.ac.ir*

ARTICLE INFO

Article history:
Received: 12 May 2013
Accepted: 23 April 2014

Keywords:
Horizontal spectrum,
Vertical spectrum,
Near field,
Forward directivity effect,
Filing step,
UBC 97,
Eurocode 8.

ABSTRACT

Recently, concerning failure of structures due to earthquakes, special investigations of near fault ground motions have been noticed. Hence, in this paper, characteristics of near field ground motions have been considered in horizontal and vertical directions. In this consideration, the record averages have been compared with Uniform Building Code and Eurocode8 spectra in two levels. In addition, the ratio of vertical to horizontal spectra has been computed and compared with the assumed value of two thirds in some code provisions. Finally, the response of near field records on five artificial bridges that have covered all 0.5-2.5 seconds periods, have been investigated for comparing the ratio of responses in near field to far field, and forward to backward directivity effects. In addition, the results of the response spectrum analyses of six different bridges subjected to vertical excitations are presented.

1. Introduction

Annually occurring in different parts of the world, earthquake is one of the most destructive catastrophes, which leads to diverse damages in structures and transportation facilities. In order to design an earthquake resistant structure, it is necessary to learn the behavior of the structure during the earthquake. Modeling, either numerical or experimental, makes it possible to monitor the behavior of the structure during the earthquake; also, the post-earthquake assessment of the ruined structures is amongst the best ways of observing the performance of different structures. The latter

approach is an important method in investigation of the conditions of built structures, especially bridges. By gathering data from the destroyed bridges during the earthquakes of ChiChi (1999), Northridge (1994), Kobe (1995), Kocaeli (1999), and Duzce (1999) it is possible to classify the causes of damage based on their abundance [17].

According to Fig. 1, the causes of damage might be traced to the structural defects and proximity to active faults. Concerning the defects, it might be said that during the recent earthquakes most of the structural problems have been properly examined and the necessary corrections have been entered in building codes. Whereas, regarding to proximity to faults, there is still no clear results to conclude which will be the main target in this paper. Besides, researchers drew attention to the significance of studying vertical ground motion and its damaging effects on structures. The importance of earthquake vertical motion to structures and the inadequacy of related studies especially in near-field regions have motivated researchers to further investigate the characteristics of vertical ground motion. On account of rarely including the effects of vertical accelerations in design of bridges for seismic loads, the objective of this study is to examine the characteristics of vertical spectrum and its effect on dynamic responses of bridges based on the available data in near-field regions. The significance of several earthquakes in recent researches was the basis of their selection in this study. Accordingly, the distance from fault was divided into six boundaries; <5, 5-10, 10-15, 15-20, 20-30 and 30-40 km from surface projection of fault rupture, and the recorded information of earthquakes was classified based on this category [11]. Through the further steps of present study, because of the probability of soil type effects on characteristics of vertical component in near field regions, records with similar soil type (soil type C based on USGS classification (1997), Average shear wave velocity to a depth of 30m 180 to 360 m/s) were included in this investigation alone. It should be mentioned that the abundance of the data in soil type C was the only reason for choosing the mentioned soil type in this investigation [27].

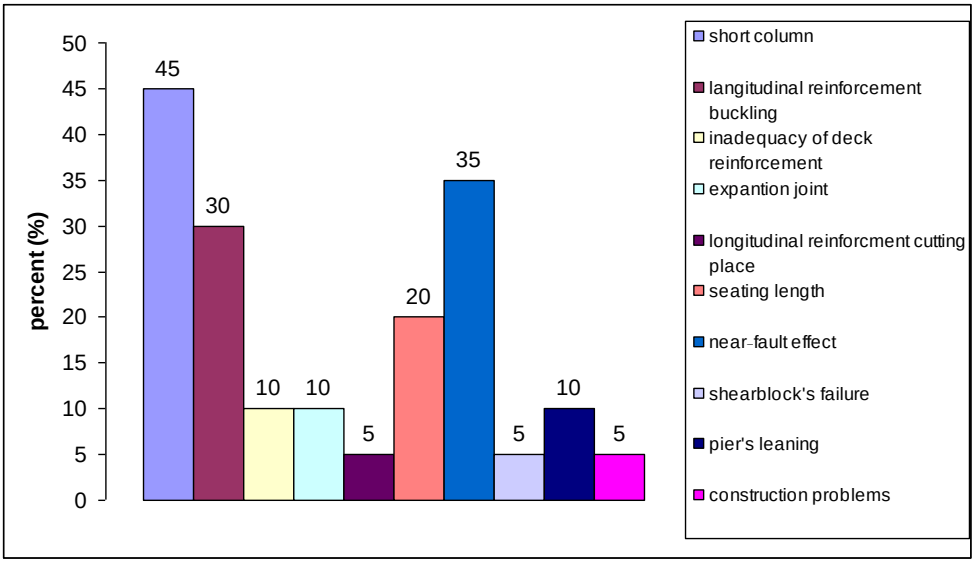

Fig. 1. Failure of bridges reason's in recent earthquake [17]

2. Near-field ground motions description

The characteristics of near-field ground motions surprisingly differ from those of far-field ground motions. When the rupture propagates toward the site and the direction is aligned with the site, large amplitude pulses with short duration and long periods emerge in recorded ground motions [24,25]. This phenomenon is called forward directivity effect and usually occurs where the velocity of rupture propagation is close to the shear-wave velocity.

Fling step is the other characteristic of near-field ground motions that stems from the residual ground displacement as a consequence of tectonic deformation. It is generally characterized by a unidirectional large-amplitude velocity pulse and the monotonic step in the displacement time history. Being in the direction of fault slip, the occurrence of fling step is not together with the forward directivity effect and arises in strike slip faults in the strike-normal direction as in the Kocaeli and Duzce earthquakes (1999) or in the strike-normal direction for dip-slip faults as in the ChiChi earthquake (1999) [1].

Permanent ground deformations in the case of fling motion would be of little consequence if they happen slowly, unless a structure straddled the fault [12]. Whether the particular slip in fling motion is rapid or not is evidenced by the duration of these displacements related to the characteristic slip time of a point on the fault [13]. Therefore, both static displacements as in fling step and shear-wave displacements as in forward directivity emerge as pulses. For moderate magnitude earthquakes, amplitude of near-field ground accelerations, velocities, and displacements can be quite high especially in the records having forward directivity. Peak accelerations may exceed 1.0 g, while peak velocities may exceed 2.0 m/sec, and peak displacements can go beyond 2.0 m.

Fig. 2 indicates the velocity and displacement time histories of the typical near-field ground motions having forward directivity and fling-step effects in comparison with that of ordinary far-field motion. There are distinctive high velocity pulses for Rinaldi record (Northridge 1995) as well as the apparent tectonic deformation at the end of the displacement time history of the ground motion recorded at SKR station (Kocaeli 1999) [19].

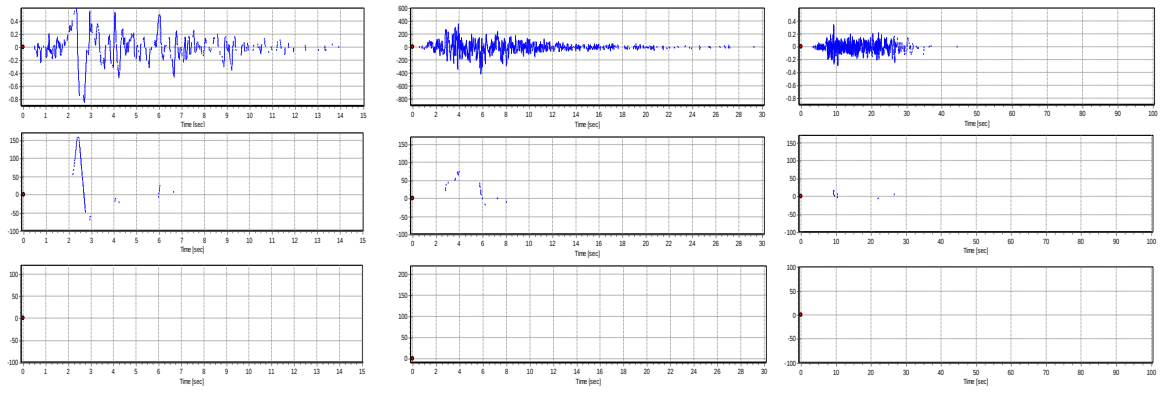

(a) (b) (c)

Fig. 2. (a) Near field and forward directivity (Rinaldi Northridge), (b) Near field and fling step (Sakarya Duzce), (c) Far field (delta Imperial Valley)

3. Characteristics of horizontal response spectra in near filed regions and its comparison with UBC97 and eurocode8's horizontal spectra

The spectra of UBC97 code design varies based on two parameters of regional soil type and the distance from fault; where the distance from the fault is applied as an increasing coefficient of them [26]. In Eurocode8 the only effective parameter is the regional soil type. In this research according to the selected records that have been registered predominantly in soil type C (USGS), the spectra of UBC97 have been assigned for soil type D and Distance less than 2 km from the fault and Eurocode8 spectra is assigned to soil type B that with shear wave velocity are coincident to soil type C (USGS) [9].

That the normal fault direction of the earthquake is stronger than the parallel one is the most conspicuous feature in near field ground motions. It is more recognizable where the rupture propagation velocity is close to the shear-wave velocity. This characteristic might be observed in different earthquakes with different magnitudes. (Fig. 3)

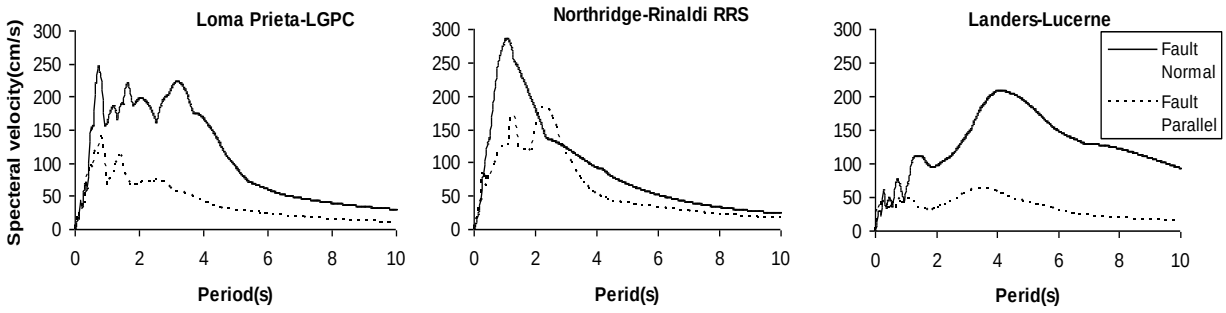

Fig. 3. Comparison between normal and parallel-to-the-fault response spectra

Obtained in near field regions, the records with fling steps are another feature that seems noteworthy to researchers. There is a static displacement in the last part of these records that is due to half-sinusoidal velocity pulses. Table 1 represents a number of these records. In order to make a comparison between the response spectra obtained from these records and the design spectra from UBC97 and Eurocode8, they have been placed in a diagram (Fig. 4). To compare the chosen records with the spectra of UBC97 and Eurocode8 code designs, the average of their spectra, and also their average and standard deviation summation (if the data is normalized it will cover 86% of the total data) has been used. It can be inferred from the diagram that the permanent static displacement has nothing to do with the response spectra and perhaps the only impact attributable to the displacements might be observable in the structures exactly placed in proximity to active faults alone.

Table 1. Ground motion records with directivity effect and fling step [19]

No.	Year	Earthquake	Mw	Station	Comp	PGA(g)	PGV(cm/s)	PGD(cm)	Fling Disp(cm)
Near-Fault Recordings (Fling-Step)									
1	1999	Kocaeli	7.4	Sakarya	EW	0.41	82.05	205.93	186.76
2	1999	Chi-Chi	7.6	TCU052	NS	0.44	216	709.09	697.12
3	1999	Chi-Chi	7.6	TCU068	EW	0.5	277.56	715.82	601.84
4	1999	Chi-Chi	7.6	TCU074	EW	0.59	68.9	193.22	174.56
5	1999	Chi-Chi	7.6	TCU084	NS	0.42	42.63	64.91	59.43
6	1999	Chi-Chi	7.6	TCU0129	NS	0.61	54.56	82.7	67.54
Near-Fault Recordings (Forward-Rupture Directivity)									
7	1989	Loma Prieta	7	LGPC	0	0.56	94.81	41.13	-
8	1989	Loma Prieta	7	Lexington Dam	90	0.41	94.26	36.66	-
9	1992	Cape Mendocino	7.1	Petrolia	90	0.66	60.26	28.89	-
10	1992	Erzincan	6.7	Erzincan	EW	0.5	64.32	21.93	-
11	1994	Northridge	6.7	Rinaldi	275	0.84	174.79	48.96	-
12	1994	Northridge	6.7	Olive View	360	0.84	130.37	31.72	-
13	1995	Kobe	6.9	KJMA	0	0.82	81.62	17.71	-

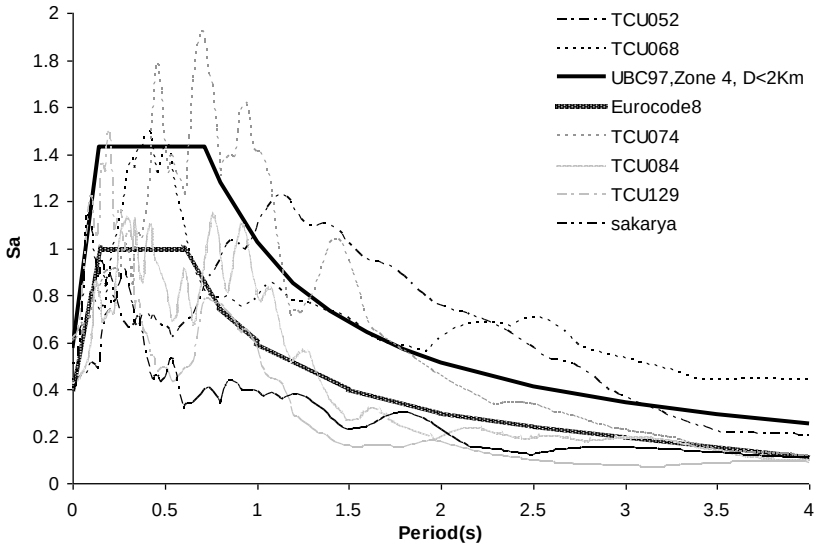

Fig. 4. Comparison between design spectra from building codes and response spectra obtained from the records with static displacements (fling step)

Concerning to the near-field records, what has an influential impact on the response spectrum is the directivity effects of the records. According to the large, observable velocity pulses in these records, it is expectable to have stronger response spectra [15,16]. In this respect, a number of records having forward directivity effect have been presented in Table 1 To compare the chosen records with the spectra of UBC97 and Eurocode8 code designs, the average of their spectra, and also their average and standard deviation summation (if the data is normalized it will cover 86% of the total data) has been used. Moreover, Fig. 5 represents the response spectra of these records compared to the design spectra of UBC97 and Eurocode8. Although, with reference to this comparison, it can be said that the average response spectra from these

records is compatible with the design spectra, the average spectra added to standard deviation (sigma), which is a basis for making logical decisions in engineering, is incompatible with the design spectra in that the peak acceleration of them is higher than that of the design spectra by a factor of 1.5. It should be mentioned that the comparison was made after applying the near-field coefficients to the spectrum of UBC97 code design, which means that the maximum, probable acceleration has been considered for the spectra in near-field regions.

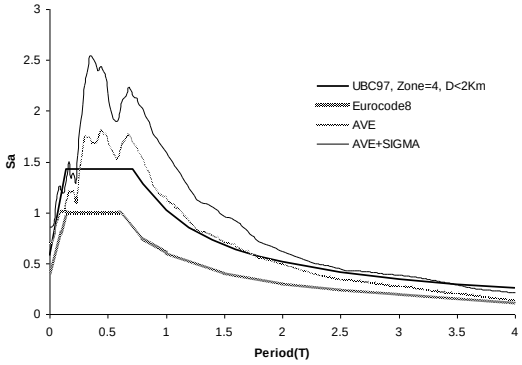

Fig. 5. Comparison between the response obtained from the records with forward directivity effect and design spectra from UBC97 and Eurocode8.

At last, the average response spectra obtained from 69 various records in 13 different earthquakes have been compared with the design spectra (Table 2). In fact, the average spectra represent the characteristics of various ground motions in near-field regions up to 15 km from the faults. The comparison indicates that the peak acceleration of the design spectra (UBC97) with applied near-field coefficients for zone 4 and distance less than 2 km is in harmony with the acceleration of the obtained average spectra added to standard deviation (sigma). However, the level of the peak acceleration in the response spectra is unvarying above the 2 sec and with the increase in period there is no significant change in the level of spectra inasmuch as in the period 4 sec the level of response is twice a level of building code's spectra (UBC97 and Eurocode8). Though, it happens in average spectra of various earthquakes, there is no evidence of its happening in average spectra obtained from Northridge earthquake. However, Northridge records have been a basis in determining the spectrum of the UBC97. (Fig. 6-b)

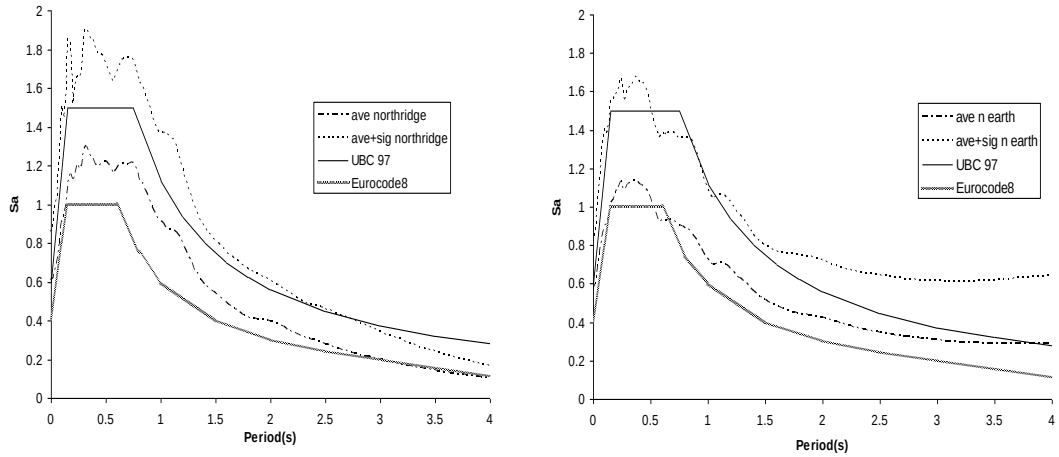

Fig. 6. Comparison of the average response spectra in near field regions and the average response spectra of Northridge earthquake with design spectra from UBC97 and Eurocode8

Table 2. Ground motion records from near fault regions

No.	Station	Comp	PGA (g)	PGV (cm/s)	PGD (cm)	Dist (km)
Parkfield (1966), M(6.1)						
1	Cholame #2	65	0.476	75.1	22.49	0.1
2	Cholame #5	85	0.442	24.7	5.15	5.3
3	Temblor	5	0.357	21.5	3.87	9.9
Sanfernando (1971), M(6.6)						
4	Pacoima Dam	164	1.226	112.5	35.50	2.8
Imperial Valley (1979), M(6.5)						
5	Bonds Corner	230	0.775	45.9	14.89	2.5
6	EC Array #3	140	0.266	46.8	18.92	9.3
7	EC Array #4	140	0.485	37.4	20.23	4.2
8	EC Array #5	230	0.379	90.5	63.03	1.0
9	EC Array #6	230	0.439	109.8	65.89	1.0
10	EC Array #7	230	0.463	110	44.74	0.6
11	EC Array #8	140	0.602	54.3	32.32	3.8
12	EC Array #9	180	0.313	29.8	13.32	8.3
13	EC Differential	360	0.48	40.8	14.04	5.3
14	EC County	92	0.235	68.8	39.35	7.6
15	EC Meloland	270	0.296	90.5	31.71	0.5
16	SAHOP	270	0.506	30.9	5.64	8.4
17	Aeropuerto	45	0.327	42.8	10.10	8.5
18	Brawley Airport	315	0.22	38.9	13.46	8.5
19	Holtville	225	0.253	48.8	31.54	7.5
Morgan Hill (1984), M(6.2)						
20	Cayot Lake Dam	285	1.298	80.8	9.63	0.1
21	Anderson Dam	250	0.423	25.3	4.58	2.6
Nahanni (1985), M(6.8)						
22	Site 1	280	1.096	46.1	14.58	6.0
23	Site 2	240	0.489	29.3	7.61	8.0
Superstitn Hill (1987), M(6.7)						
24	Parachute	225	0.455	112	52.80	0.7
25	Superstition Mtn	135	0.894	42.2	7.30	4.3
26	Poe Road	270	0.446	35.7	8.80	12.4
Loma Prieta (1989), M(6.9)						
27	Gilory Array#3	0	0.555	35.7	8.21	14.4
28	Capitola	0	0.529	36.5	9.11	14.5
29	Corralitos	0	0.644	55.2	10.88	5.1
30	Bran	0	0.453	51.3	8.37	10.3
31	LGPC	0	0.563	94.8	41.18	6.1
32	Aloha Ave	0	0.512	41.2	16.21	13
Landers (1992), M(7.3)						
33	Lucerne	275	0.721	97.6	70.31	1.1
34	Joshua Tree	90	0.284	43.2	14.51	11.6
Northridge (1994), M(6.7)						
35	Arleta	90	0.34	40.6	15.04	9.2
36	New Hall	360	0.59	97.2	38.05	7.1
37	Olive View	360	0.84	129.6	32.68	6.4
38	La Dam	64	0.51	63.7	21.18	2.6
39	Saticoy St	180	0.48	61.5	22.06	13.3
40	Sepulveda	280	0.75	84.8	18.68	8.9
41	Sylmar	52	0.61	117.4	53.47	6.2
42	Pacoima Kagel	360	0.43	51.5	7.21	8.2
43	Sun Valley	90	0.44	38.2	10.04	12.3
44	Jensen	292	0.59	99.3	24.00	6.2
45	N.Hollywood	180	0.3	25.0	6.46	14.6
46	Newhall	46	0.46	92.8	56.64	7.1
47	Pacoima Dam DS	175	0.42	45.6	5.06	8.0
48	Pacoima Dam	194	1.29	103.9	23.80	8.0
49	Rinaldi	228	0.84	166.1	28.78	7.1
Kobe (1995), M(6.9)						
50	KJMA	0	0.82	81.3	17.7	0.6
51	Takarazuka	90	0.69	85.3	16.8	1.2
52	Takatori	0	0.61	127.1	35.8	0.3
53	Nishi-Akashi	0	0.51	37.3	9.52	11.1
54	Shin-Osaka	0	0.24	37.8	8.54	15.5
Duzce (1999), M(7.1)						
55	Duzce	270	0.54	83.5	51.6	8.2
56	Lamont	375-N	0.97	36.5	5.48	8.2
Kocaeli (1999), M(7.4)						
57	Sakarya	90	0.38	79.5	70.5	3.1
58	Yarimca	330	0.35	62.1	51	2.6
59	Duzce	180	0.31	58.8	44.1	12.7
Chi-Chi (1999), M(7.6)						
60	CHY080	W	0.97	107.5	18.6	7.0
61	TCU052	W	0.35	159	184	0.2
62	CHY101	N	0.9	102.4	34	11.2
63	TCU084	W	1.16	114.7	31.4	10.4
64	TCU065	W	0.81	126.2	92.6	1.0
65	TCU068	W	0.57	176.6	324	1.1
66	TCU129	W	1.01	60	50.2	1.2
67	WNT	E	0.96	68.8	31.1	1.2
68	TCU071	N	0.66	69.4	49.1	4.9

4. Characteristics of recorded vertical motions variation of PVA with distance

Peak Vertical Acceleration is one of the most commonly used parameters to characterize ground motion [8, 23]. In order to find the relationship between PVA and distance to fault, it is essential for the records to be presented with respect to distance from fault (Figure 7). Based on Figure 1, the closer the distance of station to fault, the higher level of PVA its record contains. With the help of SeismoSignal (2006) program, the time-history acceleration of these records was converted to response spectra with 5 percent damping. Consequently, the elastic response of structure was considered in this study alone [22].

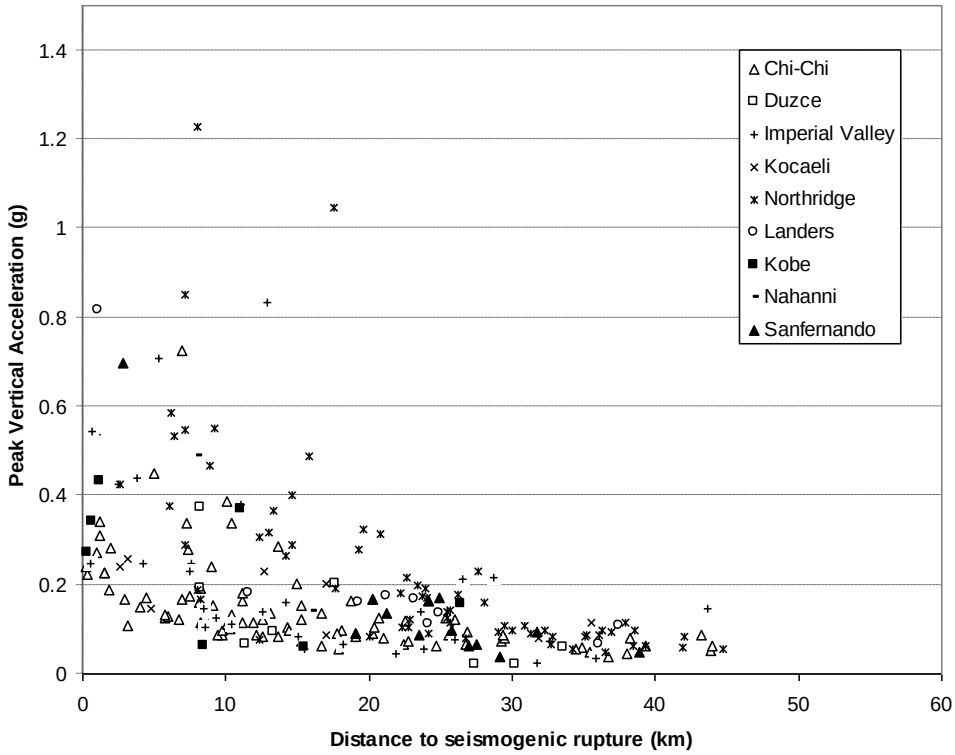

Figure 7. Variation of Peak Vertical Acceleration with respect to distance

5. Average and total average spectrum through classified distances

In order to examine the content of records with respect to their shape, quantity and distance from fault, the average spectrum for each earthquake was separately and respectively computed in classified boundaries. Finally, the total average spectrum was calculated from average spectra obtained in previous section for all earthquakes in each boundary. The Juxtaposition of the total average spectra reveals the following observations; 1) the maximum content of energy in graphs occurs between 0.03s and 0.6 s (Fig. 8). 2) With increase in distance from fault, the maximum level of acceleration in total average spectra diminishes. This process has been shown in Fig. 9.

Table 3. Earthquakes from the Pacific Earthquake Engineering Research Center

Event Name	Magnitude	Number of Available Records, by closest distance from fault (km)						
		<5	5-10	10-15	15-20	20-30	30-40	0 – 40
Landers, USA 1992/06/28	7.4	1	-	1	1	5	2	10
Chi-Chi, Taiwan 1999/09/20	7.6	18	18	17	12	18	14	97
Duzçe, Turkey 1999/11/12	7.1	1	3	2	2	1	2	11
Imperial Valley, USA 1979/10/15	6.9	8	9	7	3	5	3	35
Kocaeli, Turkey 1999/08/17	7.4	3	-	1	2	-	2	8
Northridge, USA 1994/01/17	6.7	9	9	6	8	22	21	75
Kobe, Japan 1995/01/16	6.9	3	1	1	1	1	-	7
Nahanni, Canada 1985/12/23	6.9	2	-	-	1	-	-	3
Sanfernando, USA 1978/09/16	6.6	1	-	-	3	10	2	16

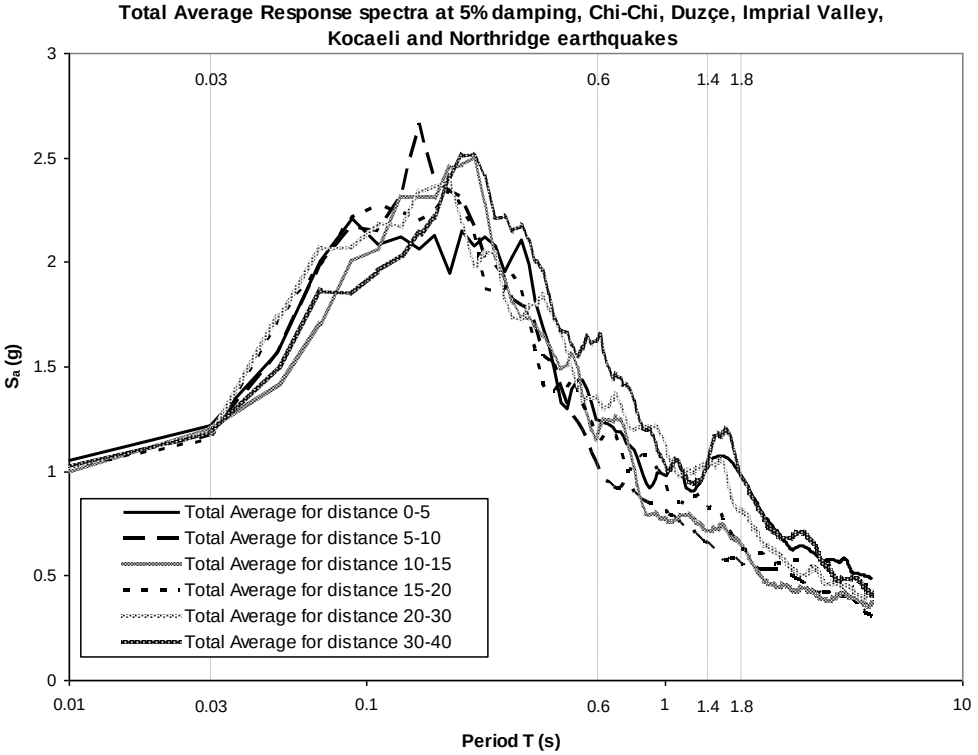

Fig. 8. Maximum content of energy in vertical spectra

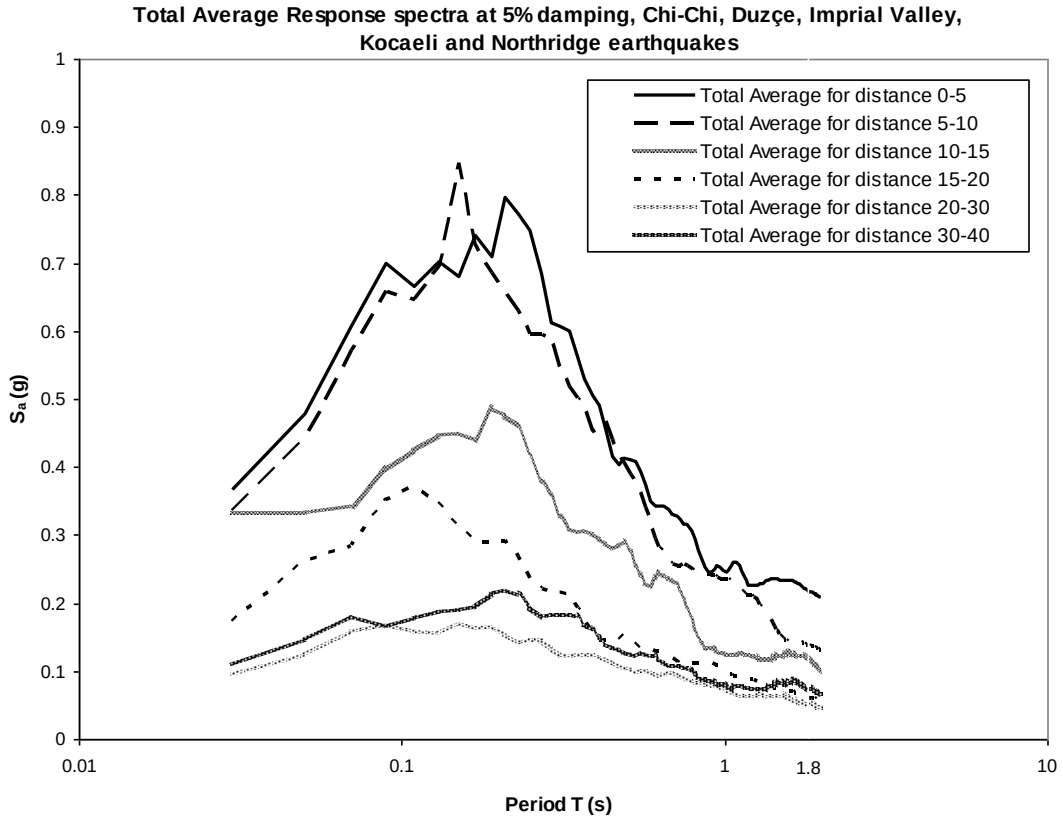

Fig. 9. Level of acceleration in total average spectra in classified boundaries

In order to find the ratio of variation of spectra in near-field regions, it is necessary to compare the spectra in these regions with the ones obtained from far-field areas. As a result, because of the insignificance change between spectra obtained in 30 and 40 km from fault, this boundary was considered as far-field. Consequently, the change in value of other total average spectra was evaluated in proportion to far field. Based on this comparison, for the first time, the average value of the acceleration-constant domain (predominant period, 0.05 to 0.4 s) of each spectrum was compared to the far-field spectrum. Subsequently, the average of entire values of each spectrum (0 to 5 s) was appraised concerning far field average value. (Table 4)

Table 4. Ratio of average spectra to far field

Spectrum	0-5 km	5-10 km	10-15 km	15-20 km	20-30 km
30-40 km (0.05 to 0.4 s)	4.49	3.92	2.42	1.59	1.14
30-40 km (0 to 5 s)	3.49	2.82	1.96	1.34	1.07

6. The ratio of vertical to horizontal response spectra

The ratio of vertical to horizontal (V/H) response spectra has been found to be strongly dependent on period and site distance from seismic source. At high frequencies the V/H spectra ratio significantly exceeds the commonly assumed ratio of 2/3 for site distances up to 40 km.

the closer the site to the source, the higher the exceedance [18]. At long periods, V/H ratio is shown to be lower [2-7]. Thus, the factor of 2/3 underestimates the effects of vertical motion at short periods and overestimates the effects at long periods. (Fig. 10)

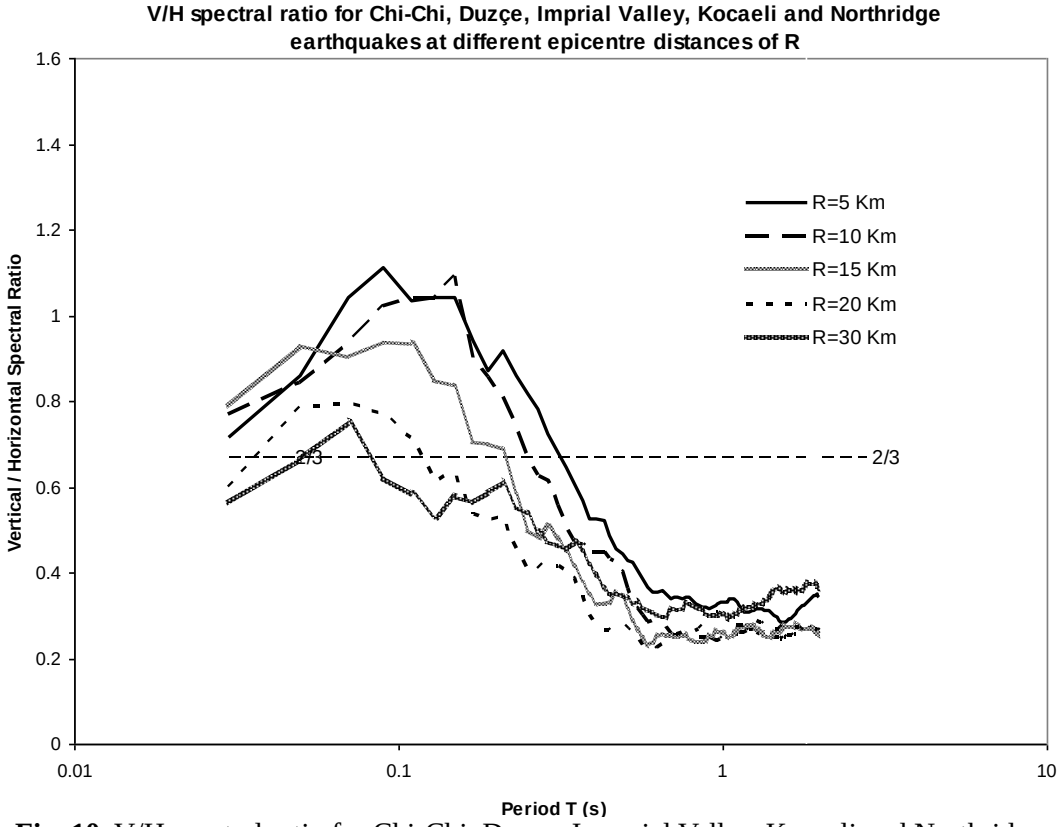

Fig. 10. V/H spectral ratio for Chi-Chi, Duzçe, Imperial Valley, Kocaeli and Northridge

7. Comparison of vertical and horizontal average spectra

Subsequent to computing the vertical average spectra, it is the time for the average horizontal spectra to be obtained from available data. Observations from both obtained average horizontal and vertical spectra would lead to the following consequences; 1) maximum acceleration occurs at incipient stage (very short periods, 0.03 to 0.6 s) of the vertical spectra in comparison to the horizontal in which the maximum acceleration happens at periods between 0.1 and 2.5 s (Fig. 11). 2) Maximum content of energy boundary in vertical spectra is much shorter than the boundary in horizontal spectra. It means the velocity spectra (commonly assumed as damage potential) deviated from horizontal is much longer in time than the one obtained from vertical spectra, and, consequently, much more destructive than the vertical velocity spectra [10].

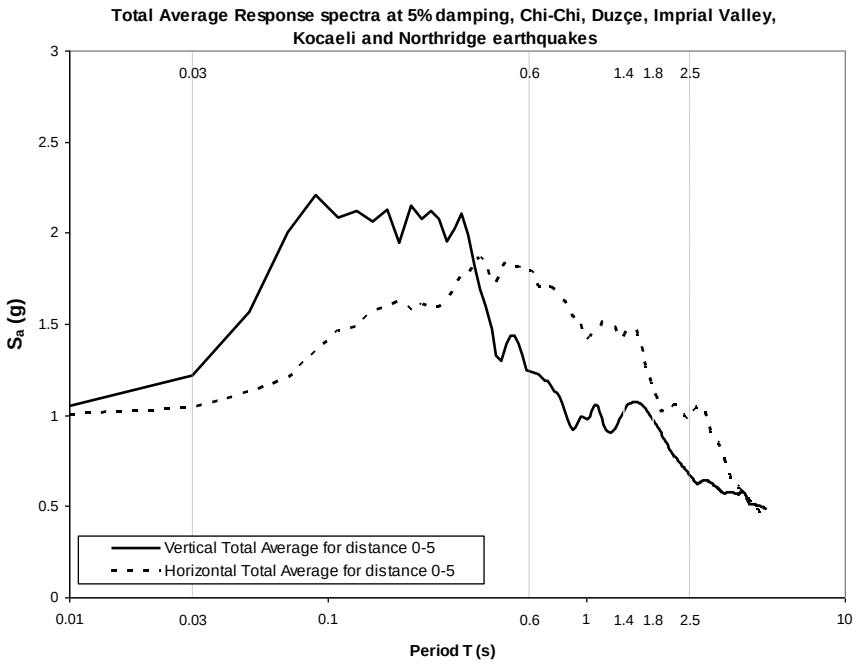

Figure 11. Comparison of vertical and horizontal average spectrum

8. Comparison of total average spectra, UBC97 specification and the vertical spectrum of European code of practice within near-field region

In order to specify the vertical effects of earthquakes within near-field regions, UBC (1997) and Eurocode8 have provided some recommendations. There is no any defined vertical spectral shape in current design codes and when the vertical component is included, it is normally specified as a spectrum based on the horizontal spectrum. To consider the 2/3 of the amplitude of horizontal spectrum after applying the near-field coefficients provided in version 1997 is the recommendation of UBC to specify the vertical spectrum [14]. Besides, Eurocode8 (2001) have provided a vertical spectrum separate from horizontal spectra. Only by comparing these spectra, the consistency and compatibility of them can evidently be represented. Therefore, at the outset, the recommended UBC spectra (soil type S_D compatible with the obtained data) for distances less than 2 km, 5 and 10 km from fault were respectively depicted in a diagram versus average vertical spectra obtained in this study (Figs. 12 to 14). Thereafter, Eurocode8's vertical spectra compared to the average spectra in another diagram. The consequences of this comparison portend of incongruity between UBC and average spectra. This inconsistency can be interpreted by the fact that the recommended vertical spectrum in UBC is fundamentally relied on the basis of horizontal spectrum which is quite different with the essence of vertical spectrum (predominant period in vertical spectrum takes place earlier than horizontal spectrum). On the other hand, despite the time coincidence of predominant periods in Eurocode8 vertical spectrum and the average, there is a considerable difference between the

levels of acceleration within near-field regions, so that the level of acceleration in average spectrum is significantly higher than the level in Eurocode8's spectrum (Fig. 15).

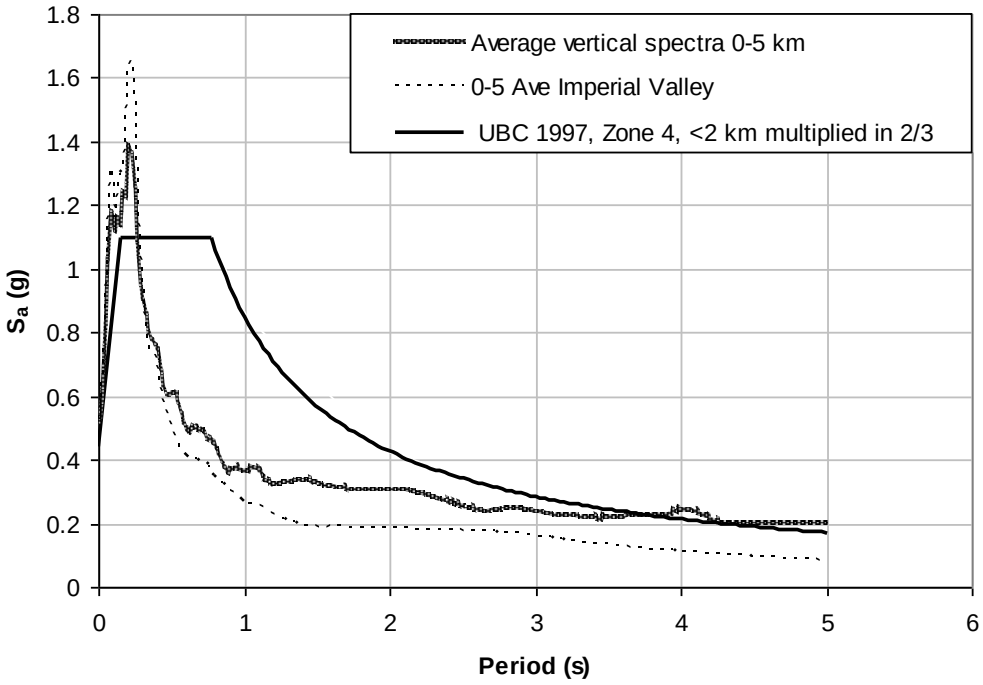

Fig. 12. 2/3 of UBC's horizontal spectrum (< 2 km) versus vertical average spectrum in < 5 km

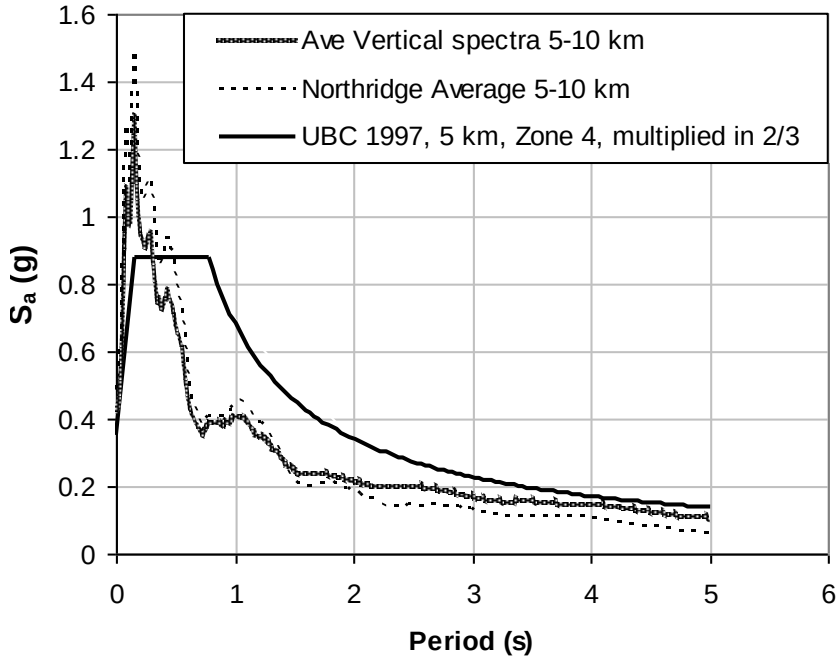

Fig. 13. 2/3 of UBC's horizontal spectrum (5 km) versus vertical average spectrum in 5-10 km

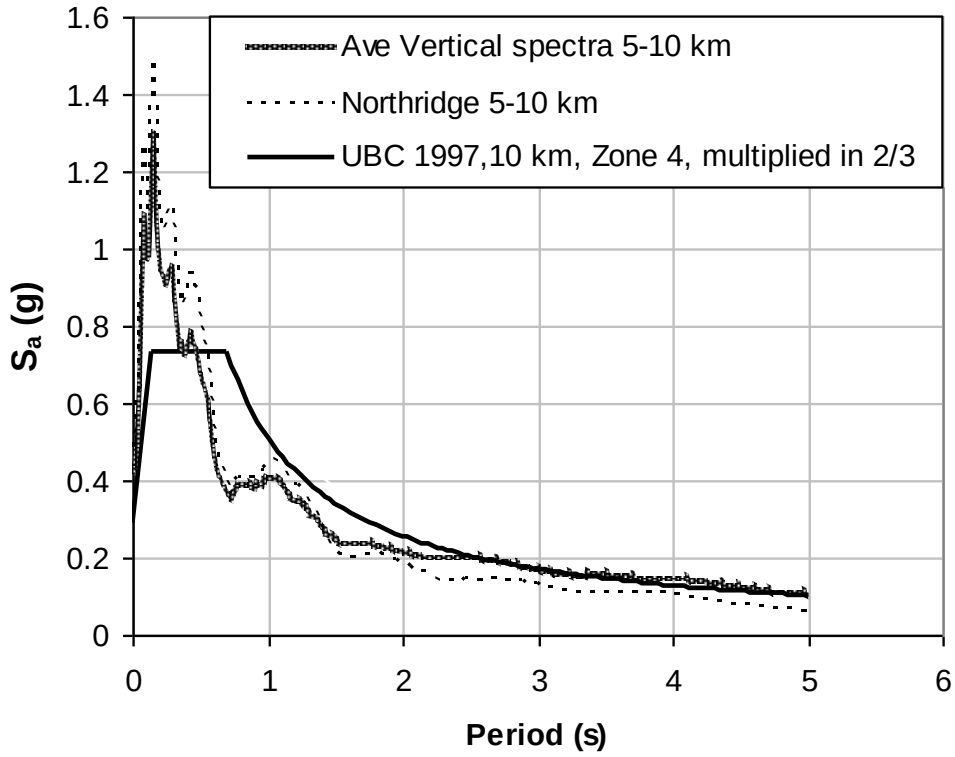

Fig. 14. 2/3 of UBC's horizontal spectrum (10 km) versus vertical average spectrum in 5-10 km

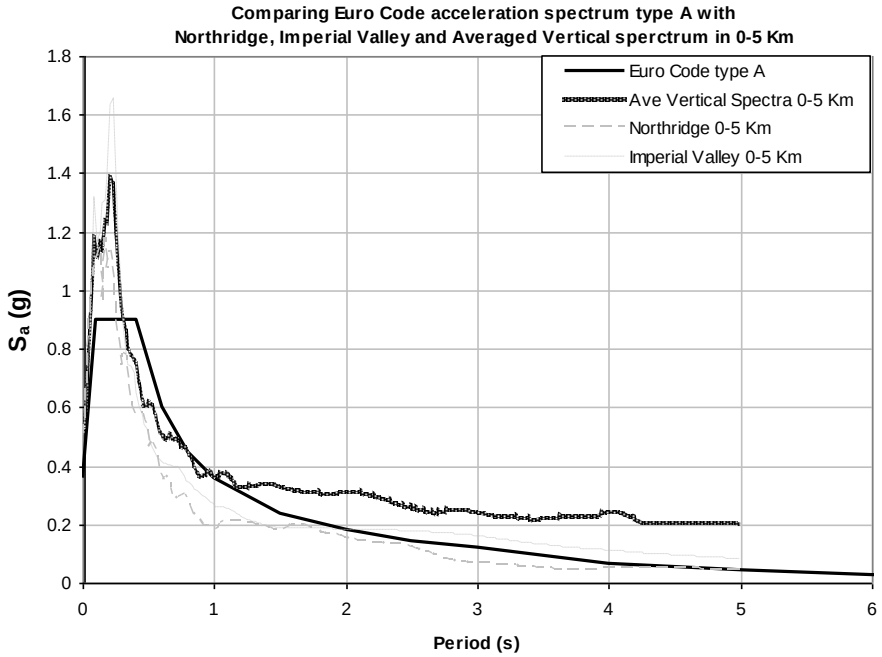

Fig. 15. Eurocode8's vertical spectrum versus vertical average spectrum in < 5 km

9. Investigation of horizontal and vertical motion effects on response of bridges in near-field region

In this section, the response of near field records on 5 artificial bridges that have covered all 0.5 - 2.5 seconds periods, have been investigated for comparing the ratio of responses in near field to far field, and forward to backward directivity effects. In addition, the results of the response spectrum analyses of six different bridges subjected to vertical excitations are presented.

9.1. Description of the modeled bridges on horizontal responses

By considering the objective of modeling and investigating of the miscellaneous urbane bridges, all the bridges used in this study are unreal and were designed by the author to be merely compared under the influence of the earthquakes. All these bridges have a concrete deck with the span of 20 m supported by three-column comprised piers with 1.5 m diameter Placed on a 1.6m × 1.6 m cap beam, the deck has a 12 m width and consists of 7 concrete girders and slabs placed in every 2 m. These bridges modeled in finite-element commercial software [21]. Table 5 presents the specifications of the modeled bridges.

Table 5. Description and properties of bridges. (horizontal motion)

Model No.	Pier Height (m)	Number of Span	Span's length (m)	Vibration's Period (S)
1	7.5	5	20	0.51
2	12	5	20	1.06
3	15	5	20	1.5
4	18	5	20	2
5	21	5	20	2.53

9.2. Analyzing the modeled bridges

With regard to the tremendous unseating due to inadequate support width, the displacement of the deck was taken into consideration and was compared in these two cases:

I. comparing the response of the bridges under the near field and far field record
II. comparing the responses under the influence of near field records having forward directivity effects and neutral records

It should be mentioned that all of the gathered records have been scaled to 0.4 g before being applied to the models. Furthermore, every pair of selected records has been chosen from same earthquake until reduced uncertainty in this analysis. At the first case, 9 pairs of record on near and far field region have been compared and, the second case, 12 pairs of record on forward and backward directivity effect have been contrasted (Table 6). In all, 140 Time history analysis were conducted. Lateral

displacement of bridge models on longitudinal direction is used as the primary measure of seismic demand.

Table 6. Ground motion records (horizontal motion)

No.	Station	Comp	PGA (g)	PGV (cm/s)	PGD (cm)	Dist (km)	Station	Comp	PGA (g)	PGV (cm/s)	PGD (cm)	Dist (km)
a. Near field and Far field												
Sanfernando (1971), M(6.6)												
1	Pacoima Dam	164	1.226	112.5	35.50	2.8	Lake Hughes	21	0.37	17	1.65	20.3
Tabas (1978), M(7.4)												
2	Tabas	TR	0.85	121.4	94.6	3.0	Dayhook	TR	0.406	26.5	8.8	17.0
Imperial Valley (1979), M(6.5)												
3	EC Array #5	230	0.379	90.5	63.03	1.0	Delta	352	0.351	33.0	19.0	43.6
4	EC County	92	0.235	68.8	39.35	7.6	Superstition Mtn	135	0.195	8.8	2.8	6.2
Northridge (1994), M(6.7)												
5	New Hall	360	0.59	97.2	38.05	7.1	Santa susana	90	0.290	19.7	7.45	19.3
Kobe (1995), M(6.9)												
6	Takatori	0	0.611	127.1	35.77	0.3	Kakogawa	90	0.345	27.6	9.6	26.4
Chi-Chi (1999), M(7.6)												
7	TCU052	W	0.348	159	184.4	0.2	TCU095	N	0.712	49.1	24.5	43.4
8	CHY101	N	0.902	102.4	33.97	11.2	TCU045	N	0.512	39.0	14.3	24.1
b. Near field (forward Directivity) and (Neutral)												
Parkfield (1966), M(6.1)												
1	Cholame #2	65	0.476	75.1	22.49	0.1	Cholame #5	85	0.44	24.7	5.15	5.3
Imperial Valley (1979), M(6.5)												
2	EC Array #6	230	0.439	109.8	65.89	1.0	Bonds Corner	230	0.78	45.9	14.9	2.5
3	EC Array #7	230	0.463	110	44.74	0.6	EC Differential	360	0.48	40.8	14.04	5.3
4	EC Meloland	270	0.296	90.5	31.71	0.5	Holtville	225	0.25	48.8	31.54	7.5
Superstitn Hill (1987), M(6.7)												
5	Parachute	225	0.455	112	52.80	0.7	Poe Road	270	0.45	35.7	8.80	12.4
Loma Prieta (1989), M(6.9)												
6	LGPC	0	0.563	94.8	41.18	6.1	Gilory Array#3	0	0.56	35.7	8.21	14.4
Landers (1992), M(7.3)												
7	Lucerne	275	0.721	97.6	70.31	1.1	Joshua Tree	90	0.28	43.2	14.5	11.6
Northridge (1994), M(6.7)												
8	Rinaldi	228	0.838	166.1	28.78	7.1	Sepulveda	280	0.75	84.8	18.68	8.9
9	Sylmar	52	0.612	117.4	53.47	6.2	Pacoima Dam	194	1.29	103.9	23.80	8.0
Kobe (1995), M(6.9)												
10	Takatori	0	0.611	127.1	35.77	0.3	Takarazuka	90	0.69	85.3	16.8	1.2
Chi-Chi (1999), M(7.6)												
11	TCU068	W	0.566	176.6	324.1	1.1	WNT	E	0.96	68.8	31.1	1.2
Duzce (1999), M(7.1)												
12	Duzce	270	0.535	83.5	51.59	8.2	Lamont	375-N	0.97	36.5	5.48	8.2

9.3. Bridges analysis results assessment

As mentioned before, modeling has been performed in order to cover periods from 0.5 to 2.5 second. First we compare near field record responses with far field ones in these models. It is necessary to mention that all these records are scaled to 0.4 g. in Fig. 16-a. we can see a sample comparison between records of imperial valley earthquake for both near and far fields for all five bridges. To compare results of the records in near and far fields they have been shown side by side on Fig. 16-b so that by fitting a line through them we could reach the average amount of near field to far field responses for every bridge.

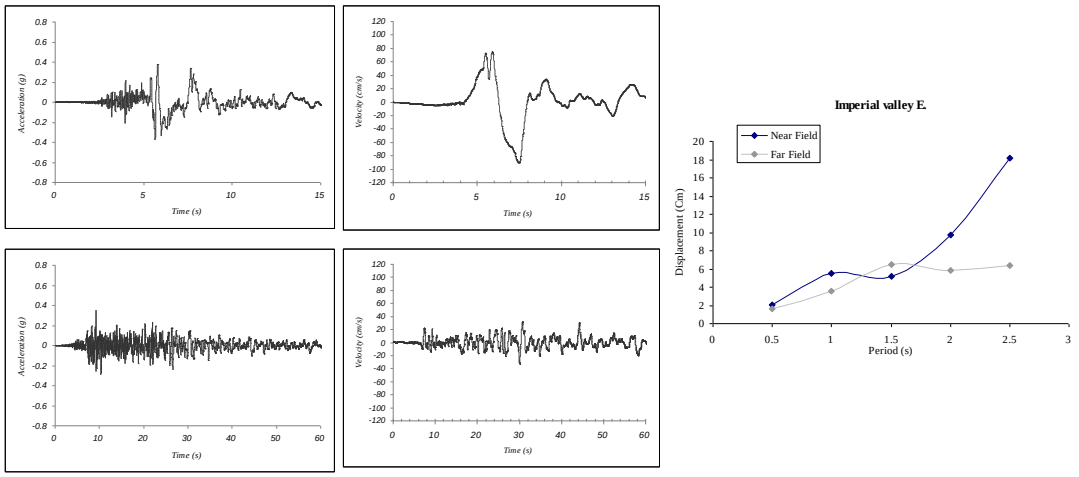

(a)

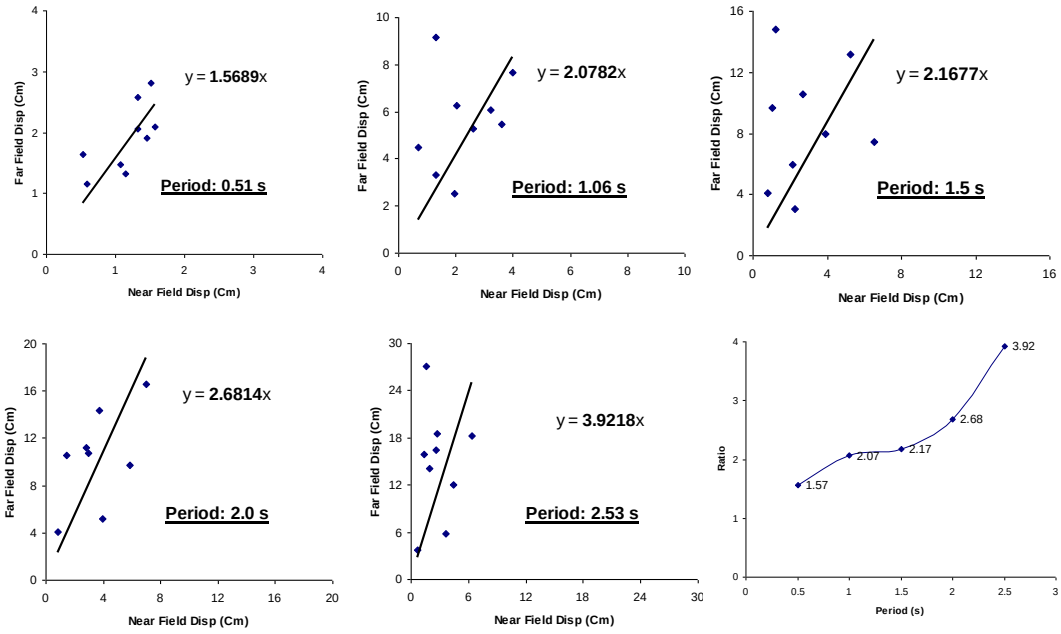

(b)

Fig. 16. (a). Comparison between Imperial valley(1979), M(6.9) Delta (PGA= .351g) Distance = 43.6 Km and ELC #5 (PGA= .379g), Distance = 1 Km
(b). The ratio of responses caused by near field to far field records

Finally, in Fig. 16-b the results of this comparison have been shown. Also in regards to near field records, the responses with forward and backward directivity effect have been compared with each other. All these records have been scaled to 0.4g. We put the results of analyses against each other for every one of these bridges and the average slope of these points are calculated. (Fig. 17)

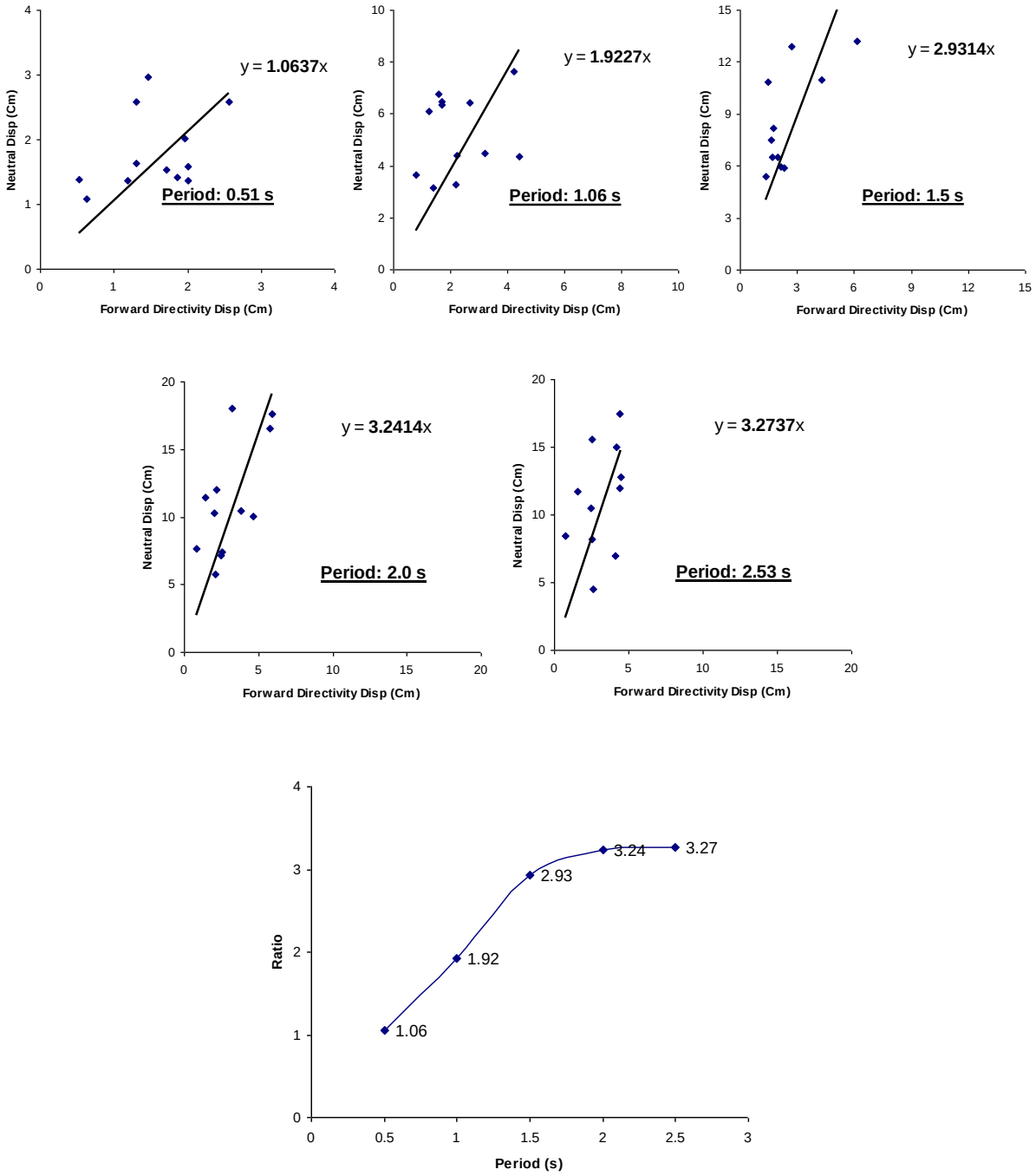

Fig. 17. The ratio of responses caused by forward to backward directivity effect on near fault regions

10. Description of the modeled bridges on vertical responses

Another objective of this study is to determine conditions in which the vertical component of seismic ground motion is critical in determining the demands placed on key elements of typical highway structures. In current design practice, the vertical component of motion is not usually included in the analysis of bridges, though the Uniform Building Code (1997) specifies increased multipliers on dead loads that are intended to approximate its effects. These multipliers are 0.9DL and 1.2DL for non-isolated buildings, and 0.8DL and 1.2DL for isolated buildings. In recent years, there has been much effort to show that the vertical-to-horizontal ratio underestimates the strength of the vertical component in the near fault region and at short periods. In present study the research approach is to analyze a representative group of bridges with a various range of natural frequencies subjected to vertical component of earthquake. The results of the dynamic analyses were compared and conclusions were drawn. The scope of the study involves linear analysis of finite element models of six typical highway bridges using a broad range of input spectra [20]. For each bridge, response spectrum analysis was performed, and results compared. Descriptions of bridge number 1 through 6 are given in Table 7. The description of each bridge includes the overall physical dimension and structural materials.

Table 7. Description and properties of Bridges 1 to 6

Bridge No.	Description	Super structure type	Span length (m)	Deck depth (m)	Deck width (m)	Moment of inertia about 3 axis (m^3)	Cross section area (m^2)	T (s)
Bridge 1	Single span	AASHTO Precast Concrete Girder	21.34	1.37	13.41	1.1626	5.67	0.201
Bridge 2	Three-span Continuous	CIP concrete	36.58 30.48	1.83	13.12	3.43	6.635	0.303
Bridge 3	Three-span Continuous	CIP concrete Box	22.4 44.8	2.56	8.8	1.7807	3.867	0.386
Bridge 4	Two-span continuous	CIP concrete Box	44.34 31.54	1.73	22.49	5.7	11.78	0.452
Bridge 5	Single span	Steel Girder	54	3.23	11.8	0.9953	0.623	0.386
Bridge 6	Single span	Steel Box	72.2	3.73	11.8	15.2696	6.13	0.755

10.1 Response spectrum analysis

Response spectrum analyses were performed on each of the six bridges using a wide range of input spectra with soil type C (S_D in UBC). Six average spectra obtained through previous sections were used to cover the range of distances <5, 10, 15, 20, 30 and 40 km. Moreover, the two-thirds of horizontal spectrum of UBC and the vertical spectrum of Eurocode8 were also applied to the bridges. The results of response spectrum analyses on the six bridges are presented in Table 8. It shows vertical bending moment quantities in the deck at the mid span and in each bridge. In multi-span bridges, responses were monitored at selective piers and spans. The format for the final presentation of results was measured by the ratio of the response of the seismic input to the dead load response. Fig. 18 shows curves for the ratio of the response of the average spectra input over the dead load only. Subsequently, Fig. 19 shows the ratio of the response of the UBC97, Erocode8, Imperial Valley and Northridge spectra input over the dead load as well.

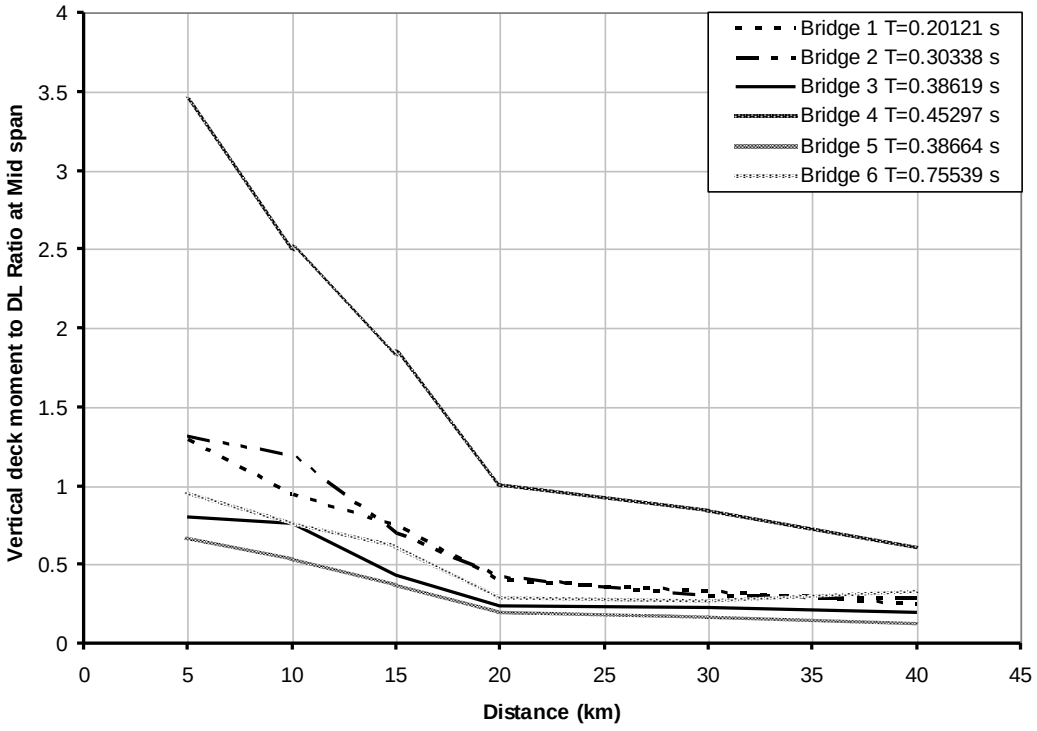

Fig. 18. The ratio of maximum vertical deck moment caused by vertical average spectra to the moment caused by DL

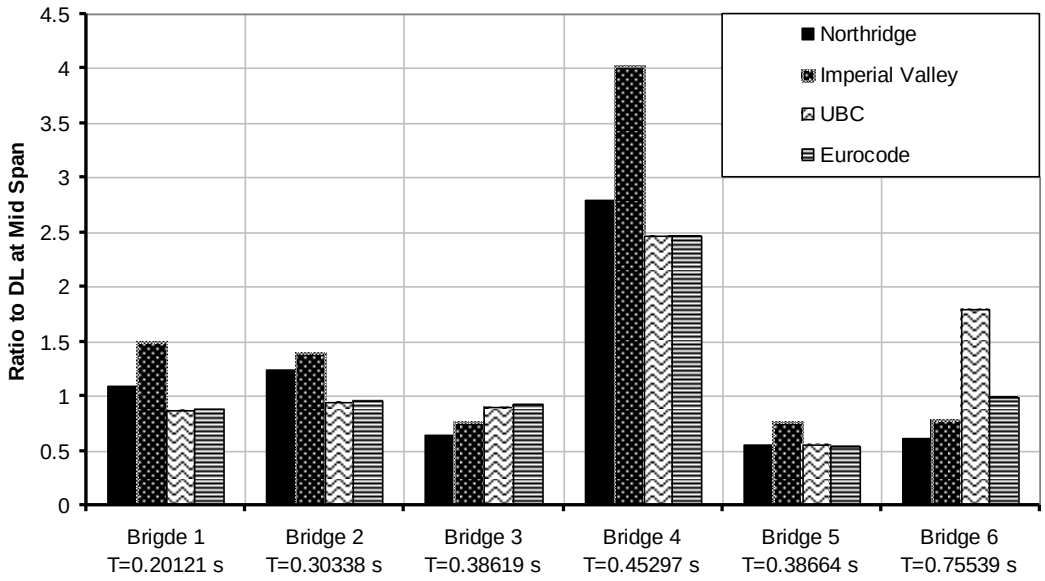

Fig. 19. The ratio of responses caused by UBC, Eurocode, Northridge and Imperial valley average spectra to the responses caused by Dead Load

Table 8 Results of response spectrum analyses and vertical moment at mid span and piers

	Bridge1		**Bridge2**		**Bridge3**		**Bridge4**			**Bridge5**		**Bridge6**	
	Mid	**Pier**	**Mid**	**Pier**	**Mid**	**Pier**	**Mid**		**Pier**	**Mid**	**Pier**	**Mid**	**Pier**
							Short Span	Long Span	-				
T(s)	0.2012		0.3034		0.3862		0.2155	0.4530	-	0.3866		0.7554	
Dead (Ton.m)	774.86	-	1060.30	1800.48	1022.65	1308.44	1192.65	4271.02	5226.73	3011.01	-	6238.03	-
0-5 km	1001.24	-	1387.18	1974.35	819.86	768.10	4103.16	2118.45	3487.58	2365.47	-	5933.98	-
5-10 km	732.91	-	1262.56	1796.91	777.95	714.86	2979.16	2994.11	2776.06	2265.03	-	4704.83	-
10-15 km	577.04	-	740.73	1054.50	440.48	423.99	2193.19	1681.83	1914.85	1256.22	-	3856.92	-
15-20 km	306.22	-	440.77	627.47	244.34	278.07	1201.39	832.20	1042.85	627.12	-	1765.24	-
20-30 km	252.88	-	320.61	456.35	225.72	208.25	999.63	697.36	858.11	650.29	-	1667.63	-
30-40 km	187.67	-	300.39	427.57	203.31	186.95	726.10	684.33	666.10	589.43	-	2027.98	-
Northridge Average	846.15	-	1311.34	1866.48	651.45	645.69	3335.6	2446.63	2892.67	1822.93	-	3862.96	-
Imperial Valley Average	1160.22	-	1476.62	2101.62	786.01	750.09	4801.66	2707.29	3985.40	2247.88	-	4849.88	-
UBC 1997	669.43	-	995.51	1416.82	917.78	799.71	2946.65	3446.79	2876.80	2734.49	-	11200.00	-
Eurocode	684.66	-	1018.17	1449.12	943.75	833.40	2945.07	2867.30	2818.35	2796.90	-	6164.93	-

10. Conclusion

In most cases of near field records, the normal component is more intensive than the parallel component in the fault.

The parallel component of near field fault records, if the fault is a strike slip, create a sudden pulse which can be seen repeatedly in the seismographs. This phenomenon does not have much effect on the response spectrum.

In near field records that are bound to a direction, the response spectrum is much greater than the UBC97 design code spectrum which reaches values up to 1.5 times the maximum.

The horizontal spectrum calculated from the average values of near field record spectrum of different earthquakes us bi different than the UBC97 spectrum when it comes to the maximum value. Only when periodic values are greater than 2 seconds, the average spectrum is displayed as a line with a constant value where in 4 second periods the resulting value is twice the design code.

With increasing the distance to the fault, Peak Vertical Acceleration significantly diminishes.

The maximum content of energy in vertical motions occurs in high-frequency domains or short periods between 0.03s and 0.6 s. while, this domain begins from 0.1 to 2.5 s in horizontal motion.

In near field regions, the ratio of vertical spectrum to the horizontal is more than the two-thirds of the horizontal recommended in some code provisions to specify the vertical spectrum. This ratio for the distances less than 5 km to the source can get the value more than unit and for the distances more than 15 km is much less than 2/3. It means that to consider the two-thirds of the horizontal spectra's domain as the vertical spectra seems unreasonable in near field regions.

The ratio of variation for the near-field vertical spectrum to the far field can approximately reach to the value 4 in distances less than 5 km to the fault.

The comparison of total average vertical spectrum in < 5 km and the two-thirds of the UBC 97 horizontal spectra with the same distance shows that the average spectrum contains a very short acceleration-constant domain. In addition, the average spectrum has a higher level of dominant period with respect to UBC.

The comparison of total average vertical spectrum in < 5 km and the Eurocode's vertical spectrum shows that except the incongruity in their PVA, they both have the similar acceleration-constant domain.

Based on the conclusion made between the record response of near field and far field points on bridges, it can be presumed that the ratio of record responses of near field to far field data will largely increase as the period is amplified; where this ratio is increased to 3 in a 2.5 second period.

In the case of comparing direction bound and neutral records, the same relationship is seen. Therefore, comparing near field records with no direction bounds to far field records is possible.

The closer the natural vertical period of the deck to the predominant period of the spectrum, the more the influence of the vertical motion on deck.

The ratio of maximum deck moment caused by average spectra to the moment caused by dead load is more than unit in distances less than 15 km to the source.

The mentioned ratio can reach to 3.5 for bridge No. 4. This sudden increase in deck moment stems from the fact that the bridge has asymmetrical spans and wider deck (two times) in comparison to the others that could, in turn, enhance the stiffness (rigidity) with respect to span, and consequently decrease the natural period, and intensify the effect of vertical motion.

Using the two-thirds of the UBC horizontal spectrum in analyses would cause increase in responses' quantities in bridges with the natural period more than 0.75 s. this increase is related to the fact that the acceleration-constant domain in this spectra is longer than the real vertical spectra and as a result can affect the structures with longer natural period.

References

[1] Abrahamson, N. (2001). "Incorporating Effects of Near Fault Tectonic Deformation into Design Ground Motions", a presentation sponsored by the Earthquake Engineering Research Institute Visiting Professional Program, hosted by State University of New York at Buffalo, 26 Oct. 2001. Available at http://mceer.buffalo.edu/outreach/pr/abrahamson.asp

[2] Ambarseyes, N. N., Douglas, J. (2000). "Reappraisal of the Effect of Vertical Ground Motions on Response". Engineering Seismology and Earthquake Engineering, ESEE, Report No. 00-4, Department of Civil Engineering and Environmental Engineering, Imperial College of Science, Technology and Medicine.

[3] Ambarseyes, N. N., Simpson, K. A. (1996). "Prediction of vertical response spectra in Europe". Earthquake Engineering & Structural Dynamics, Vol. 25(4), pp. 401-412.

[4] American Association of State Highway & Transportation Officials (AASHTO), (1992). Standard specifications for highway bridges, www.aashto.org.

[5] Boore, D. M., Joyner, W. B. and Fumal, T. E. (1997). "Equations for estimating horizontal response spectra and peak acceleration from western North American earthquakes: A summary of recent work". Seismological Research Letters, Vol. 68(1), pp. 128-153.

[6] Bozorgnia, Y. Niazi, M. (1993). "Distance scaling of vertical and horizontal response spectra of the Loma Prieta earthquake", Earthquake Engineering & Structural Dynamics, Vol. 22(8), pp. 695-707.

[7] Bozorgnia, Y., Niazi, M., Campbell, K. W. (1995). "Characteristic of free-field vertical ground motion during the Northridge earthquake". Earthquake Spectra, Vol. 11(4), pp. 515-525.

[8] Elgamal, A., He, L. (2004). "Vertical earthquake ground motion records: An overview". Journal of Earthquake Engineering, Vol. 5(8), pp. 663-697.

[9] European Standard (2001), Eurocode 8: Design of Structures for Earthquake Resistance, DRAFT No 4, Final Project Team Draft (Stage 34), prEN 1998-1: 200X, 1-19.

[10] Foutch, A. D., (1997). "A note on the occurrence and effects of vertical earthquake ground motion," Proceedings of the FHWA/NCEER Workshop on the National Representation of Seismic Ground Motion for New and Existing Highway Facilities, Technical Report NCEER-97-0010.

[11] Frankel, A. D., Meuller, C., Barnhard, T., Leyendecker, E., Wesson, R., Harmsen, A., Klein, F., Perkins, D., Dickman, N., Hanson, S., (2000). "USGS national seismic hazard maps". Earthquake Spectra, Vol. 16(1), pp. 1-19.

[12] Hall, J. F., Heaton, T. H., Halling, M. W., and Wald, D. J., (1995). "Near-source ground motions and effects on flexible buildings". Earthquake Spectra, Vol. 11(4), pp. 569-605.

[13] Heaton, T. H., Hall, J. F., Wald, D. J., Halling, M. W. (1995). "Response of high-rise and base-isolated buildings to a hypothetical Mw 7.0 blind thrust earthquake". Science, Vol. 267 (13), pp. 206-211.

[14] Kircher, C.A. (2003). "Development of Seismic Design Criteria for Building Codes". Kircher & Associates, Palo Alto, CA.

[15] Kalkan, E., Adalier, K., Pamuk, A., (2004). "Near field effects and engineering implications of recent earthquakes in Turkey". Proceedings, 5th International Conference on Case Histories in Geotechnical Engineering, New York, NY, April 13-17, Paper No. 3-30.

[16] Mavroeidis, G. P., and Papageorgiou, A. S., (2003). "A mathematical expression of Near-fault ground motions". Bull. Seismol. Soc. Am. 93 (3), pp. 1099-1131.

[17] Memarpour, M.M. (2005). "Investigation of failure reasons of bridges in recent earthquakes." M.Sc. Thesis, Dept of Civil Engineering, Iran University of Science and Technology, Tehran, Iran. (in Farsi)

[18] Newmark, N. M., Blume J. A., Kapur K. K., (1973). "Seismic design spectra for nuclear power plants". Journal of the Power Division, Vol.99, pp. 287-303.

[19] Pacific Earthquake Engineering Strong-Motion Databases. Available at: http://peer.berkeley.edu/smact/index.html

[20] Priestly, MJ. N., Seible, F., Calvi G. M., (1996). "Seismic Design and Retrofit of Bridges". John Wiley and Sons, Inc., New York.

[21] SAP 2000. Integrated Finite Element Analysis and Design of Structures, Version Advanced 10.01, 2005.

[22] SeismoSignal. SeismoSoft, Version 3.1.0, 2006.

[23] Silva, W. J. (1997). "Characteristics of vertical ground motions for applications to engineering design" Proceedings of the FHWA/NCEER Workshop on the National Representation of Seismic Ground Motion for New and Existing Highway Facilities, Technical Report NCEER-97-0010.

[24] Somerville, P. G., (1998). "Development of an improved representation of near-fault ground motions" SMIP98, Proceedings, Seminar on Utilization of Strong-Motion Data, Oakland, CA, Sept. 15, California Division of Mines and Geology, Sacramento, CA, pp. 1-20.

[25] Somerville, P. G., Smith, N., Graves, R., Abrahamson, N., (1997). "Modification of empirical strong motion attenuation relations to include the amplitude and duration effects of rupture directivity". Seismol, Res. Lett. Vol. 68, pp. 180-203.

[26] Uniform Building Code (UBC). (1997) International Conference of Building Officials, Structural Design Provisions.

[27] United States Geological Survey (USGS). https://www.usgs.gov/